IEEE Access
Multidisciplinary | Rapid Review | Open Access Journal

Received September 23, 2018, accepted October 15, 2018, date of publication October 23, 2018,
date of current version November 19, 2018.

Digital Object Identifier 10.1109/ACCESS.2018.2877602

Efficient Real-Valued Rank Reduction Algorithm for DOA Estimation of Noncircular Sources Under Mutual Coupling

JIAN XIE[1,2,3], (Member, IEEE), LING WANG[1,2], (Member, IEEE), AND YUEXIAN WANG[2], (Member, IEEE)

[1]Research & Development Institute of Northwestern Polytechnical University in Shenzhen, Shenzhen 518057, China
[2]Electronics and Information School, Northwestern Polytechnical University, Xi'an 710072, China
[3]Shaanxi Lingyun Electronics Group Co., Ltd., Baoji 721006, China

Corresponding author: Jian Xie (xiejian@nwpu.edu.cn)

This work was supported in part by the National Natural Science Foundation of China under Grant 61601372, in part by the Science, Technology and Innovation Commission of Shenzhen Municipality under Grant JCYJ20170306154016149 and Grant JCYJ20170815154325384, in part by the China Postdoctoral Science Foundation under Grant 2017M613200, in part by Natural Science Basic Research Plan in Shaanxi Province of China under Grant 2017JQ6068, and in part by the Shanghai Aerospace Science and Technology Innovation Fund under Grant sast2017-077.

ABSTRACT Noncircular sources are widely used in wireless communication array systems, which can offer more accurate estimates and detect more sources. However, in practical array systems, the direction-of-arrival (DOA) estimation performance may be severely degraded by mutual coupling effects. To solve this problem, we propose a real-valued DOA estimation algorithm for noncircular sources under unknown mutual coupling. Based on the sources' noncircularity, an augmented real-valued covariance matrix is constructed. Then, utilizing the banded symmetric and Toeplitz property of the mutual coupling matrix, the middle subarray elements are considered as ideal ones, which have the same array gains. Finally, according to the subspace principle, a rank reduction-based virtual steering vector parameterizing method is derived, which extracts the DOAs from other nuisance parameters. Compared with conventional algorithms, the proposed one not only improves the estimation accuracy but also resolves more sources. Moreover, it is computationally efficient, since it only requires real-valued computations and 1-D spectral search. Numerical simulations demonstrate that the proposed method performs well under unknown mutual coupling and outperforms some of the existing approaches in resolution capability, estimation accuracy, and computational loads.

INDEX TERMS DOA estimation, mutual coupling, noncircular sources, rank reduction.

I. INTRODUCTION

Directions-of-arrival (DOA) estimation by an array of sensors has been applied in many important areas, such as radar, sonar and smart city [1]. In general, most DOA estimation algorithms are based on the implicit assumption that the radiating sources are complex circular [2]. It is well known that in modern digital communication systems, noncircular signals such as binary phase shift keying (BPSK) and M-ary amplitude-shift keying (MASK) are widely used. Recently, various DOA estimation algorithms have been proposed to utilize the structure of second-order noncircularity of the sources [3]–[7]. For noncircular signals, both conjugated and unconjugated covariance matrices contain the second-order statistical characteristics. Therefore, by making use of the noncircularity, we can resolve more sources and obtain more accurate DOA estimates [8].

In [2], a noncircular MUSIC-like (NCMUSIC) method is tailored for noncircular signals, which performs better than the standard MUSIC algorithm provided that the noncircularity rate of uncorrelated sources is one. Gao *et al.* [9] and Chen *et al.*[10] further generalize the MUSIC algorithm for the DOA estimation problem of mixed circular and strictly noncircular sources. In [11], a $2q$th-order cumulants based direction finding approach is extended to noncircular

signals, which can detect more noncircular signals and outperforms the NCMUSIC algorithm. But, this method is computationally prohibitive, since it requires constructing $2q$th-order cumulants. In [12], by using overcomplete dictionaries to express the conjugated and unconjugated covariance matrices subject to sparsity constraint, the authors introduced sparse recovery technique to address the problem of DOA estimation of noncircular sources. However, it involves l_1-norm minimization problem, which is also computationally demanding. Zheng *et al.* [13] proposed an approach to jointly estimate direction of departure (DOD) and DOA in bistatic multiple input multiple output (MIMO) radar under the scenario of mixed noncircular and circular sources. Xie *et al.* [14], [15] have extended the signal model to the near-field localization problem for noncircular sources.

Generally, these techniques assume that the array manifold is ideal without any uncertainty, such as mutual coupling effects. However, in the practical applications of array systems, the mutual coupling effect is often unavoidable, which will greatly reduce or even invalidate the performance of the above direction finding algorithms.

Fortunately, many direction finding and calibration techniques have been developed to eliminate or reduce the mutual coupling effect [16]–[23]. Among these methods, calibration sources with exactly known locations are widely used to evaluate and compensate the mutual coupling effects [16], [17]. However, this kind of methods require recalibration for multiple times, and the calibration sources may be unavailable in practical systems. Alternatively, another kind of autocalibration methods are proposed, since they avoid additional calibration sources. Friedlander introduced an alternating minimization algorithm for DOA estimation and mutual coupling self-calibration [18]. However, the multidimensional spectral search cannot be applied in real-time. Recently, based on the auxiliary sensors at both ends of a uniform linear array (ULA), Ye *et al.* [19], Ye and Liu [20], Xu *et al.* [21], and Liu *et al.* [22] proposed some DOA estimation techniques that circumvent any calibration source and multi-dimensional search. Yet, the array aperture is not fully utilized in these methods, especially under strong mutual coupling effects, since only the middle subarray rather than the whole array can be used for direction finding. Liao *et al.* [23] transforms mutual coupling effect into gain and phase uncertainties of the array, where the uncertainties for the middle subarray are the same. Thereafter, utilizing the observations from the whole array, DOA and mutual coupling parameters can be obtained via rank reduction (RARE) principle. Moreover, a fourth-order cumulant (FOC) method is proposed in [26], whose performance is superior especially under the strong mutual coupling scenario. Xie *et al.* [27] proposed a RARE based algorithm to localize mixed far-field and near-field sources under mutual coupling effect.

To the best of our knowledge, there has been very limited work contributing to the DOA estimation of noncircualr signals under unknown mutual coupling. Huang *et al.* [28] only analyzed the performance of NC-MUSIC for uncorrelated strictly noncircular signals in the presence of mutual coupling, and formulated the DOA biases in a closed form. Therefore, aiming at filling this lack, we propose a real-valued direction finding algorithm for noncircular sources in the presence of mutual coupling. Traditional subspace-based DOA estimation approaches involve complex-valued computations for the covariance matrix, eigenvalue decomposition (EVD) and spectral search. Many studies have been devoted to a certain unitary transformation which converts the complex-valued information to the field of real numbers [29]–[31]. The computational load of EVD and spectral search for this kind of transformation is decreased by a factor of four. However, the transformation itself is still complex-valued and bring additional computations. Therefore, it brings us a motivation for seeking a more efficient method to relieve the computational cost of the complex-valued calculations.

Based on the noncircularity of the sources, we take the real part and the imaginary part of the array outputs to construct an extended covariance matrix. Then, the middle subarray elements of the virtual arrays are found to be ideal ones which have the same array gains. Consequently, a RARE based virtual steering vector parameterizing method is derived, which decouples the DOA estimation from other nuisance parameters. The stochastic Cramér-Rao Bound (CRB) of DOA estimation for noncircular signals under unknown mutual coupling is also derived.

The advantages of the presented method are:

1) More sources can be resolved compared with the RARE-based algorithms in [21], because of the exploitation of the noncircularity;
2) The DOA estimation accuracy can be effectively improved by exploiting signal noncircularity.
3) It is efficient since it avoids complex-valued computations and multidimensional search.

The rest of this paper is organized as follows. In Section 2, a model of noncircular signals with unknown mutual coupling is formulated. Then, the proposed direction finding algorithm is described in Section 3. Next, a comparison among the proposed algorithm and some newly developed algorithms is shown in Section 4. In Section 5, simulations are carried out to evaluate the performance of the proposed approach. Section 6 concludes our new findings in this paper. Appendix includes the detailed derivation of the stochastic CRB for the corresponding signal model.

Note that the key notations throughout the paper are listed in Table 1 for conciseness.

II. SIGNAL MODEL

Consider K narrowband and mutually independent sources radiating onto a ULA composed of M omnidirectional elements. Ideally, the array observation without mutual coupling

TABLE 1. Key notations used in this paper.

Notations	Explanation
$(\cdot)^*,(\cdot)^T,(\cdot)^H$	Conjugate, transpose and conjugate transpose
$\mathrm{Re}\{\cdot\}$	Real part operator
$\mathrm{Im}\{\cdot\}$	Imaginary part operator
$E\{\cdot\}$	Statistical expectation operator
$\mathrm{vec}(\cdot)$	Vectorization operator
$\odot,\otimes$	Hadamard-Schur product and Kronecker product
$\mathrm{Tr}\{\cdot\}$	Trace operator
$\mathbf{I}_M$	An $M\times M$ identity matrix
$\det(\cdot)$	Determinate operator
$\mathbf{\Pi}_{\mathbf{A}}^{\perp}$	Orthogonal projection matrix onto the null space of $\mathbf{A}$

is of the following form

$$\mathbf{x}(t)=\sum_{k=1}^{K}\mathbf{a}(\theta_k)s_k(t)+\mathbf{n}(t)=\mathbf{A}\mathbf{s}(t)+\mathbf{n}(t) \tag{1}$$

Herein, $\mathbf{a}(\theta_k)=[1,u(\theta_k),\ldots,u^{M-1}(\theta_k)]^T$ is the ideal steering vector with $u(\theta_k)=\exp(-j2\pi d\sin\theta_k/\lambda)$, θ_k is the DOA of the kth signal, λ is the wavelength, and d is the distance between adjacent elements which is a half wavelength to avoid phase ambiguities. $\mathbf{A}=[\mathbf{a}(\theta_1),\ldots,\mathbf{a}(\theta_K)]$ symbolizes the steering matrix of the K sources. In addition, $\mathbf{s}(t)=[s_1(t),s_2(t),\ldots,s_K(t)]^T$ is the signal vector, and $\mathbf{n}(t)=[n_1(t),n_2(t),\ldots,n_M(t)]^T$ is the noise vector, where it is assumed to be additive white Gaussian, and statistically independent of all impinging signals.

However, in practice, the electromagnetic interaction between the antenna elements may introduce a mismatched array manifold. In this scenario, the current in each antenna element of an array depends not only on their own excitation but also on the contributions from adjacent antenna elements [18]. As a result, considering the mutual coupling effect between the array elements, the associated observation vector should be modified as

$$\begin{aligned}\mathbf{x}(t)&=\mathbf{C}\mathbf{A}\mathbf{s}(t)+\mathbf{n}(t)\\&=\sum_{k=1}^{K}\bar{\mathbf{a}}(\theta_k)s_k(t)+\mathbf{n}(t)=\bar{\mathbf{A}}s(t)+\ \mathbf{n}(t)\end{aligned} \tag{2}$$

Herein, $\bar{\mathbf{a}}(\theta)=\mathbf{C}\mathbf{a}(\theta)$ and $\bar{\mathbf{A}}=[\bar{\mathbf{a}}(\theta_1),\ldots,\bar{\mathbf{a}}(\theta_k)]$ are the steering vector and array manifold matrix under mutual coupling effect, respectively. And $\mathbf{C}\in\mathbb{C}^{N\times N}$ represents the so-called mutual coupling matrix, whose entries are the mutual coupling coefficients (MCCs).

Friedlander pointed out that MCC is inversely proportional to the distance between two antenna elements [18]. Thus, the coefficients between adjacent elements are almost equal, and the coefficients approaches to zero when the elements are far away. Accordingly, $\mathbf{C}$ is a banded symmetric Toeplitz matrix with P nonzero coefficients.

$$\mathbf{C}=\begin{bmatrix}1&c_1&\cdots&c_{P-1}&0&\cdots&0\\c_1&1&c_1&\vdots&\ddots&\ddots&\vdots\\\vdots&c_1&1&\ddots&\vdots&\ddots&0\\c_{P-1}&\vdots&\ddots&\ddots&\ddots&\vdots&c_{P-1}\\0&\ddots&\vdots&\ddots&1&c_1&\vdots\\\vdots&\ddots&\ddots&\vdots&\vdots&1&c_1\\0&\cdots&0&c_{P-1}&\cdots&c_1&1\end{bmatrix} \tag{3}$$

where $c_i=\rho_i e^{j\phi_i}$ is the nonzero mutual coupling coefficient, ρ_i and ϕ_i represent the amplitude and the phase of the ith coefficient c_i, respectively.

Additionally, if the received signals are strictly second-order noncircular, the signal vector can be written as the following form [3]

$$\mathbf{s}(t)=\mathbf{\Phi}\boldsymbol{s}_0(t) \tag{4}$$

where $\mathbf{s}_0(t)=[s_{0,1}(t),\ldots,s_{0,K}(t)]^T\in\mathbb{R}^{K\times 1}$ is the real-valued signal vector, and $\mathbf{\Phi}=\mathrm{diag}\{e^{j\psi_1},\ldots,e^{j\psi_K}\}$ is a diagonal matrix which contains the noncircular phase shifts of the signals [11].

Therefore, the array observation vector for noncircular signals with mutual coupling is given by

$$\mathbf{x}(t)=\mathbf{C}\mathbf{A}\mathbf{\Phi}\mathbf{s}_0(t)+\mathbf{n}(t) \tag{5}$$

With the array observation $\mathbf{x}(t)$, this paper aims at obtaining the DOA estimation of noncircular signals under unknown mutual coupling effects.

III. PROPOSED REAL-VALUED RARE ALGORITHM

Notice that the previous works on noncircular sources DOA estimation problems directly use the conjugated counterpart of the signal to construct an extended covariance matrix, which still operates in the complex domain [9]–[14]. In fact, based on the noncircular characteristics of the sources, the real part and imaginary part of the received signal can also be concatenated to construct a real-valued augmented data matrix, which can be proceeded in the real domain [15].

A. EXTENDED REAL-VALUED SIGNAL MODEL

In order to conduct the transformation of the complex-valued data to real-valued domain, we have the real and imaginary parts of $\mathbf{x}(t)$, respectively, as

$$\mathbf{x}_R(t)=\mathrm{Re}[\mathbf{x}(t)]=[\mathbf{x}(t)+\mathbf{x}^*(t)]/2 \tag{6}$$

$$\mathbf{x}_I(t)=\mathrm{Im}[\mathbf{x}(t)]=[\mathbf{x}(t)-\mathbf{x}^*(t)]/2j \tag{7}$$

According to the signal model in (5), we further have

$$\begin{aligned}\mathbf{x}_R(t)&=\left(\mathbf{C}\mathbf{A}\mathbf{\Phi}+\mathbf{C}^*\mathbf{A}^*\mathbf{\Phi}^*\right)\mathbf{s}_0(t)/2+\mathrm{Re}\left[\mathbf{n}(t)\right]\\&=\bar{\mathbf{A}}_R\mathbf{s}_0(t)+\mathbf{n}_R(t)\end{aligned} \tag{8}$$

$$\begin{aligned}\mathbf{x}_I(t)&=\left(\mathbf{C}\mathbf{A}\mathbf{\Phi}-\mathbf{C}^*\mathbf{A}^*\mathbf{\Phi}^*\right)\mathbf{s}_0(t)/2j+\mathrm{Im}\left[\mathbf{n}(t)\right]\\&=\bar{\mathbf{A}}_I\mathbf{s}_0(t)+\mathbf{n}_I(t)\end{aligned} \tag{9}$$

where $\bar{\mathbf{A}}_R = [\mathbf{v}_R(\theta_1, \psi_1, \mathbf{C}), \ldots, \mathbf{v}_R(\theta_K, \psi_K, \mathbf{C})]$ and $\bar{\mathbf{A}}_I = [\mathbf{v}_I(\theta_1, \psi_1, \mathbf{C}), \ldots, \mathbf{v}_I(\theta_K, \psi_K, \mathbf{C})]$ are the virtual steering matrices of $\mathbf{x}_R(t)$ and $\mathbf{x}_I(t)$, respectively. While $\mathbf{n}_R(t)$ and $\mathbf{n}_I(t)$ represent the real and imaginary parts of the noise vector $\mathbf{n}(t)$. Therefore, the virtual steering vector of $\mathbf{x}_R(t)$ can be expressed as

$$\begin{aligned}\mathbf{v}_R(\theta_k, \psi_k, \mathbf{C}) &= \mathbf{C}\mathbf{a}(\theta_k) \cdot e^{j\psi_k} + \mathbf{C}^*\mathbf{a}^*(\theta_k) \cdot e^{-j\psi_k} \\ &= h_c(\theta_k, \psi_k, \mathbf{C})\boldsymbol{\Gamma}_c(\theta_k, \psi_k, \mathbf{C})\mathbf{a}_c(\theta_k) \\ &\quad - h_s(\theta_k, \psi_k, \mathbf{C})\boldsymbol{\Gamma}_s(\theta_k, \psi_k, \mathbf{C})\mathbf{a}_s(\theta_k) \quad (10)\end{aligned}$$

where

$$\mathbf{a}_c(\theta) = [1, \cos u(\theta), \cos 2u(\theta), \ldots, \cos(M-1)u(\theta)]^T \quad (11)$$

$$\mathbf{a}_s(\theta) = [0, \sin u(\theta), \sin 2u(\theta), \cdots, \sin(M-1)u(\theta)]^T \quad (12)$$

$$h_c = \sum_{i=1-P}^{P-1} \rho_{|i|} \cos\left(\phi_{|i|} + \psi_k + i \cdot u_k(\theta)\right) \quad (13)$$

$$h_s = \sum_{i=1-P}^{P-1} \rho_{|i|} \sin\left(\phi_{|i|} + \psi_k + i \cdot u_k(\theta)\right) \quad (14)$$

$$\boldsymbol{\Gamma}_c = diag\left[\alpha_1^{(c)}, \ldots, \alpha_{P-1}^{(c)}, 1, \ldots, 1, \beta_1^{(c)}, \ldots, \beta_{P-1}^{(c)}\right] \quad (15)$$

$$\boldsymbol{\Gamma}_s = diag\left[\alpha_1^{(s)}, \ldots, \alpha_{P-1}^{(s)}, 1, \ldots, 1, \beta_1^{(s)}, \ldots, \beta_{P-1}^{(s)}\right] \quad (16)$$

Herein, $\boldsymbol{\Gamma}_c$ and $\boldsymbol{\Gamma}_s$ are both $M \times M$ diagonal matrices containing $M - 2P + 2$ ones between the elements $\alpha_{P-1}^{(c)}$ and $\beta_1^{(c)}$ (also between $\alpha_{P-1}^{(s)}$ and $\beta_1^{(s)}$). From (13) and (14), it can be seen that h_c and h_s are two scalar parameters related to the DOAs, noncircular phases and mutual coupling coefficients. In general, they are assumed to be non-zero. And for $p = 1, 2, \ldots, P-1$,

$$\alpha_p^{(c)} = \frac{h_c - \sum_{i=p}^{P-1} \rho_i \cos\left(\phi_i + \psi_k - i \cdot u(\theta_k)\right)}{h_c} \quad (17)$$

$$\alpha_p^{(s)} = \frac{h_s - \sum_{i=p}^{P-1} \rho_i \sin\left(\phi_i + \psi_k - i \cdot u(\theta_k)\right)}{h_s} \quad (18)$$

$$\beta_p^{(c)} = \frac{h_c - \sum_{i=P-p}^{P-1} \rho_i \cos\left(\phi_i + \psi_k + i \cdot u(\theta_k)\right)}{h_c} \quad (19)$$

$$\beta_p^{(s)} = \frac{h_s - \sum_{i=P-p}^{P-1} \rho_i \sin\left(\phi_i + \psi_k + i \cdot u(\theta_k)\right)}{h_s} \quad (20)$$

Similarly, the virtual steering vector of $\mathbf{x}_I(t)$ can be expressed as

$$\begin{aligned}\mathbf{v}_I(\theta_k, \psi_k, \mathbf{C}) &= \mathbf{C}\mathbf{a}(\theta_k) \cdot e^{j\psi_k} - \mathbf{C}^*\mathbf{a}^*(\theta_k) \cdot e^{-j\psi_k} \\ &= h_s(\theta_k, \psi_k, \mathbf{C})\boldsymbol{\Gamma}_c(\theta_k, \psi_k, \mathbf{C})\mathbf{a}_s(\theta_k) \\ &\quad + h_c(\theta_k, \psi_k, \mathbf{C})\boldsymbol{\Gamma}_s(\theta_k, \psi_k, \mathbf{C})\mathbf{a}_c(\theta_k) \quad (21)\end{aligned}$$

Based on the above analysis, we can now construct a real-valued augmented data matrix

$$\begin{aligned}\mathbf{y}(t) &= \begin{bmatrix}\mathbf{x}_R(t) \\ \mathbf{x}_I(t)\end{bmatrix} = \begin{bmatrix}\bar{\mathbf{A}}_R \\ \bar{\mathbf{A}}_I\end{bmatrix}\mathbf{s}_0(t) + \begin{bmatrix}\mathbf{n}_R(t) \\ \mathbf{n}_I(t)\end{bmatrix} \\ &= \mathbf{A}_E\mathbf{s}_0(t) + \mathbf{n}_E(t) \quad (22)\end{aligned}$$

where $\mathbf{A}_E = [\mathbf{a}_E(\theta_1, \phi_1, \mathbf{C}), \mathbf{a}_E(\theta_2, \phi_2, \mathbf{C}), \ldots, \mathbf{a}_E(\theta_K, \phi_K, \mathbf{C})]$ is the extended steering matrix with the extended real-valued steering vector being

$$\mathbf{a}_E(\theta_k, \psi_k, \mathbf{C}) = \begin{bmatrix}\mathbf{v}_R(\theta_k, \psi_k, \mathbf{C}) \\ \mathbf{v}_I(\theta_k, \psi_k, \mathbf{C})\end{bmatrix} \quad (23)$$

The real-valued covariance matrix of $\mathbf{y}(t)$ can be written as

$$\mathbf{R}_y = E\left\{\mathbf{y}(t)\mathbf{y}^T(t)\right\} = \mathbf{A}_E\mathbf{R}_{S_0}\mathbf{A}_E^T + \sigma_n^2\mathbf{I}_{2M} \quad (24)$$

where $\mathbf{R}_{S_0} = E\{\mathbf{s}_0(t)\mathbf{s}_0^T(t)\}$, $\mathbf{I}_{2M}$ is a $2M \times 2M$ identity matrix. By taking the eigenvalue decomposition of $\mathbf{R}_\mathbf{y}$, we further have

$$\mathbf{R}_y = \mathbf{U}_s\boldsymbol{\Lambda}_s\mathbf{U}_s^H + \sigma_n^2\mathbf{U}_n\mathbf{U}_n^H \quad (25)$$

where $\boldsymbol{\Lambda}_s$ contains largest K eigenvalues on its diagonal. $\mathbf{U}_s$, a $2M \times K$ matrix, includes K eigenvectors and spans the signal subspace of $\mathbf{R}_y$, and $\mathbf{U}_n$, a $2M \times (2M\text{-}K)$ matrix, includes $2M$-K eigenvectors and spans the noise subspace of $\mathbf{R}_y$.

In view of the orthogonality between the signal subspace and noise subspace, multidimensional MUSIC method can be utilized for the joint estimation of DOAs, noncircular phases and mutual coupling coefficients:

$$P(\theta, \psi, \mathbf{C}) = \mathbf{a}_E^T(\theta, \psi, \mathbf{C})\,\mathbf{U}_n\mathbf{U}_n^T\mathbf{a}_E(\theta, \psi, \mathbf{C}) \quad (26)$$

It is noticeable that this estimator is computationally prohibitive since it requires a $P + 2$ dimensional spectral search. To reduce the computational load, a real-valued rank reduction algorithm is proposed in the next subsection, which decouples the DOA estimation from other nuisance parameters and therefore only involves 1-D spectral search.

B. RANK REDUCTION FOR DOA ESTIMATION

In this subsection, a novel steering vector parameterization method is introduced considering the special structure of the mutual coupling matrix—banded symmetric as well as Toeplitz [18].

According to (10) and (21), the mutual coupling effect in both virtual steering vectors can be viewed as gain and phase perturbations related to angles. Fortunately, the diagonal matrices $\boldsymbol{\Gamma}_c$ and $\boldsymbol{\Gamma}_s$ contain a vector whose elements are all ones, which implies that the middle subarray can be deemed as an ideal one without any perturbation. Using this property, the virtual steering vectors in (10) and (21) can be parameterized as

$$\mathbf{v}_R(\theta, \psi, \mathbf{C}) = \mathbf{T}_c(\theta)\boldsymbol{\alpha}_c(\theta, \psi, \mathbf{C}) - \mathbf{T}_s(\theta)\boldsymbol{\alpha}_s(\theta, \psi, \mathbf{C}) \quad (27)$$

$$\mathbf{v}_I(\theta, \psi, \mathbf{C}) = \mathbf{T}_c(\theta)\boldsymbol{\alpha}_s(\theta, \psi, \mathbf{C}) + \mathbf{T}_s(\theta)\boldsymbol{\alpha}_c(\theta, \psi, \mathbf{C}) \quad (28)$$

where $\mathbf{T}_c(\theta)$ and $\mathbf{T}_s(\theta)$ are $M \times (2P-1)$ block diagonal matrices, α_c and α_s are $(2P-1)\times 1$ real vectors, which are given by

$$\mathbf{T}_c(\theta) = \begin{bmatrix} 1 & & & & \\ & \cos(\theta) & & \mathbf{0} & \\ & & \ddots & & \\ & & & \cos((P-1)\theta) & \\ & & & \vdots & \\ & \mathbf{0} & & \cos((M-P)\theta) & \\ & & & & \ddots \\ & & & & & \cos((M-1)\theta) \end{bmatrix} \tag{29}$$

$$\mathbf{T}_s(\theta) = \begin{bmatrix} 1 & & & & \\ & \sin(\theta) & & \mathbf{0} & \\ & & \ddots & & \\ & & & \sin((P-1)\theta) & \\ & & & \vdots & \\ & \mathbf{0} & & \sin((M-P)\theta) & \\ & & & & \ddots \\ & & & & & \sin((M-1)\theta) \end{bmatrix} \tag{30}$$

$$\boldsymbol{\alpha}_c = h_c \left[\alpha_1^{(c)}, \ldots, \alpha_{P-1}^{(c)}, 1, \beta_1^{(c)}, \ldots, \beta_{P-1}^{(c)}\right]^H \tag{31}$$

$$\boldsymbol{\alpha}_s = h_s \left[\alpha_1^{(s)}, \ldots, \alpha_{P-1}^{(s)}, 1, \beta_1^{(s)}, \ldots, \beta_{P-1}^{(s)}\right]^H \tag{32}$$

Furthermore, the extended real-valued steering vector in (23) can be rewritten as

$$\begin{aligned} \mathbf{a}_E(\theta, \psi, \mathbf{C}) &= \begin{bmatrix} \mathbf{v}_R(\theta, \psi, \mathbf{C}) \\ \mathbf{v}_I(\theta, \psi, \mathbf{C}) \end{bmatrix} \\ &= \begin{bmatrix} \mathbf{T}_c(\theta)\boldsymbol{\alpha}_c(\theta, \psi, \mathbf{C}) - \mathbf{T}_s(\theta)\boldsymbol{\alpha}_s(\theta, \psi, \mathbf{C}) \\ \mathbf{T}_c(\theta)\boldsymbol{\alpha}_s(\theta, \psi, \mathbf{C}) + \mathbf{T}_s(\theta)\boldsymbol{\alpha}_c(\theta, \psi, \mathbf{C}) \end{bmatrix} \\ &= \underbrace{\begin{bmatrix} \mathbf{T}_c(\theta) & -\mathbf{T}_s(\theta) \\ \mathbf{T}_s(\theta) & \mathbf{T}_c(\theta) \end{bmatrix}}_{\mathbf{T}(\theta)} \underbrace{\begin{bmatrix} \boldsymbol{\alpha}_c \\ \boldsymbol{\alpha}_s \end{bmatrix}}_{\boldsymbol{\alpha}(\theta,\psi,\mathbf{C})} \end{aligned} \tag{33}$$

Substituting (33) into (26), we have

$$\boldsymbol{\alpha}^T(\theta, \psi, \mathbf{C})\mathbf{Q}(\theta)\boldsymbol{\alpha}(\theta, \psi, \mathbf{C}) = 0 \tag{34}$$

where

$$\mathbf{Q}(\theta) = \mathbf{T}^T(\theta)\mathbf{U}_n\mathbf{U}_n^T\,\mathbf{T}(\theta) \tag{35}$$

is a $(4P-2)\times(4P-2)$ real matrix. Note that $\mathbf{T}(\theta) \in \mathbb{R}^{2M\times 2(2P-1)}$, $\mathbf{U}_n \in \mathbb{R}^{2M\times(2M-K)}$, and $\mathbf{Q}(\theta) \in \mathbb{R}^{2(2P-1)\times 2(2P-1)}$; then if $2M-K \geq 2(2P-1)$, $\mathbf{Q}(\theta)$ is generally of full column rank. Since $\boldsymbol{\alpha}$ is assumed to be non-zero, (34) can be true only if $\mathbf{Q}(\theta)$ is rank deficient. The rank of $\mathbf{Q}(\theta)$ drops if and only if $\theta = \theta_k$, $k = 1, \ldots, K$, in terms of the idea of RARE. Thus, DOA estimation can be conducted by searching the K highest peaks from the following 1-D spectral function

$$P(\theta) = \frac{1}{\det\left[\mathbf{T}^T(\theta)\mathbf{U}_n\mathbf{U}_n^T\mathbf{T}(\theta)\right]} \tag{36}$$

Notice that θ is now decoupled from the nuisance parameters $\mathbf{C}$ and ψ. As a result, the computational complexity of the proposed RARE estimator is significantly reduced compared with the MUSIC algorithm, since it only requires real-valued operation and 1-D spectral search.

C. IMPLEMENTATION OF THE ALGORITHM

Note that the exact covariance matrices and subspaces are utilized in the previous subsections, but the theoretical covariance matrix like $\mathbf{R}_y$ in (24) is unavailable due to the limited snapshots. In practice, it can be estimated as

$$\hat{\mathbf{R}}_y = \frac{1}{T}\sum_{t=1}^{T}\left\{\mathbf{y}(t)\mathbf{y}^T(t)\right\} \tag{37}$$

Consequently, the presented DOA estimation algorithm is summarized as follows.

Step 1. Extract the real and imaginary parts of the received data vector $\mathbf{x}(t)$ via (6) and (7);
Step 2. Construct a real-valued augmented data matrix $\mathbf{y}(t)$ based on (22);
Step 3. Estimate the real-valued covariance matrix $\mathbf{R}_y$ using (37);
Step 4. Eigendecompose $\mathbf{R}_y$ to generate its noise subspace $\mathbf{U}_n$ as in (25);
Step 5. Construct the matrix $\mathbf{T}(\theta)$ for each searching step according to equations (29), (30) and (33);
Step 6. Estimate the DOAs through the spatial spectrum function obtained from the real-valued RARE estimator in (36).

IV. DISSCUSSION

A comparison of our technique with some state-of-the-art DOA estimation methods under mutual coupling effect is given in this section: the auxiliary sensors based algorithm (AUX) in [20], the rank reduction based algorithm (RARE) in [23] and the fourth-order cumulant (FOC) based algorithm in [26].

A. COMPUTATIONAL COMPLEXITY

The computational complexity analysis is based on the main multiplications required in the development of statistical matrices, EVDs and spectral search. Assume that an M-element array is used by all these algorithms. The searching step of the spectral function is designated as θ_Δ. AUX constructs a $(M-2P+2)\times(M-2P+2)$ covariance matrix, performs the EVD and spectral search. RARE requires building an $M\times M$ covariance matrix, taking EVD and 1-D spectral search. FOC builds $(M-2P+2)$ fourth order cumulant matrices of the same size $M\times M$, and requires implementing the SVD of a $(M-2P+2)M\times M$ cumulant matrix. For the proposed one, it needs to establish a $2M\times 2M$

TABLE 2. Computational complexity comparison.

Method	Statistical Matrices	EVDs	Spectral Search
AUX	$O(4(M-2P+2)^2T)$	$O(4(M-2P+2)^3/3)$	$O(720(M-2P+2)^2/\theta_\Delta)$
RARE	$O(4M^2T)$	$O(4M^3/3)$	$O(720M^2/\theta_\Delta)$
FOC	$O(36(M-2P+2)M^2T)$	$O(4M^3(M-2P+2)^3/3)$	-
Proposed	$O(4M^2T)$	$O(8M^3/3)$	$O(180M^2/\theta_\Delta)$

real-valued covariance matrix, perform EVD on this matrix and executing 1-D spectral search. It should be noticed that all these operations involved in the proposed algorithm are processed in the real domain. Therefore, with the same matrix dimension, the proposed method can effectively decrease the computational complexity by a factor of four. The comparison results are listed in Table 2.

B. MAXIMUM NUMBER OF RESOLVABLE SOURCES

In this subsection, we discuss the maximum number of resolvable sources of these algorithms for a given ULA with M elements. For AUX, it only uses the $M-2P+2$ elements in the middle of the array. Since the subspace-based methods must use at least one eigenvector to span the noise subspace, AUX can handle $M-2P+1$ sources at most. Likewise, RARE can resolve $M-2P+1$ sources simultaneously. FOC takes full use of the array aperture, and therefore it can estimate up to $M-1$ sources. For the proposed algorithm, the noncircularity of the signal has been exploited to construct an extended subspace, thus it can resolve up to $2(M-2P+1)$ sources, which is doubled compared with RARE.

V. SIMULATION RESULTS

In this section, a series of numerical simulations are carried out to compare the performance of the proposed algorithm with other four methods (NCMUSIC, AUX, RARE and FOC). We adopt a ULA with 10 elements in the simulations and assume that $d=\lambda/2$. The incident signals are independently BPSK modulated with an equal power. The algorithms are evaluated through spectrum, probability of resolution (PR), root mean-square error (RMSE) and computational complexity. The PR is the ratio between the times of signals being successfully resolved to the total number of Monte Carlo runs. Let Δ denote the angular separation between the two sources with incident angles $\theta_k, k=1,2$. They are said to be correctly resolved if the DOA estimates satisfy $\left|\theta_k-\hat{\theta}_k\right| < \Delta/2$. The RMSE is defined as

$$RMSE=\sqrt{\frac{1}{500}\sum_{n=1}^{500}\left(\theta_k-\hat{\theta}_{n,k}\right)^2}$$

where θ_k is the DOA of the kth source, and $\hat{\theta}_{n,k}$ stands for the estimate of θ_k in the nth trial.

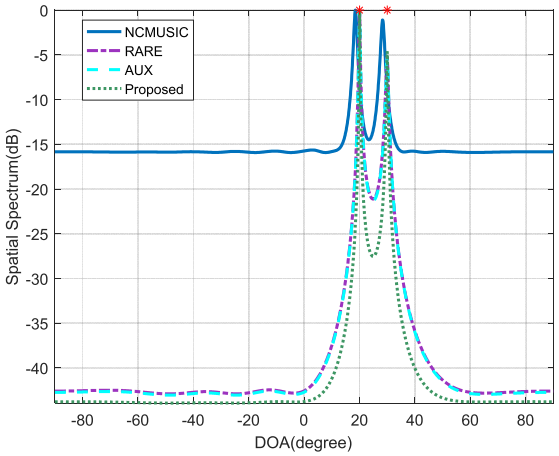

FIGURE 1. DOA spectra obtained with NCMUSIC, AUX, RARE and the proposed method for two BPSK sources. The sources are impinging from 20° and 30°.

A. SPECTRA OF DOA ESTIMATORS UNDER MUTUAL COUPLING

In this experiment, the spectra of NCMUSIC, AUX, RARE and the proposed algorithm under mutual coupling are investigated.

First, we assume that there are two uncorrelated BPSK sources radiating from 20° and 30°, with the signal-to-noise ratio (SNR) and the number of snapshots being 10 dB and 200, respectively. Because the mutual coupling effect reduces as the distance between two sensors increases, the nonzero MCCs is set as $[1, 0.37+j0.42, 0.09-j0.31]$ (i.e., $P=3$).

The normalized DOA spectra of the four methods are shown in Fig. 1. It can be seen that the DOA estimates indicated by NCMUSIC spectrum have obvious biases due to the perturbations of array manifold generated from mutual coupling. However, for the other three methods, two sharp peaks point to the true DOAs of both signals, since the mutual coupling effect has been compensated in proper ways by these methods. Moreover, the spectrum peaks generated by the proposed method are much sharper than those of AUX and RARE, which indicates the improvement of the estimation accuracy due to the exploitation of noncircularity.

Next, we increase the number of radiating BPSK sources to 10, with their DOA parameters being $-70°$, $-55°$, $-40°$, $-25°$, $-10°$, $5°$, $20°$, $35°$, $50°$ and $65°$. In this scenario, the AUX and RARE would fail since they can only handle $M-2P+1$ sources at most. Therefore, we only depict the spectra of NCMUSIC and the proposed method in Fig.2. The proposed algorithm can accurately obtain all DOA estimates, while the spectral peaks of NCMUSIC are biased and thus less reliable.

B. RMSE VERSUS SNR

In this experiment, the relationship of the estimation accuracy with the SNR is evaluated under mutual coupling effect. Assume that there are three uncorrelated BPSK sources

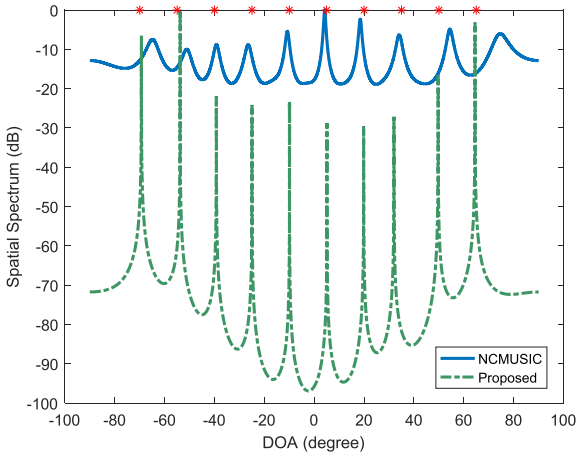

FIGURE 2. DOA spectra obtained with NCMUSIC and the proposed method for ten BPSK sources. The sources are impinging from −70°, −55°, −40°, −25°, −10°, 5°, 20°, 35°, 50° and 65°. (Note that the number of array elements is only 10.)

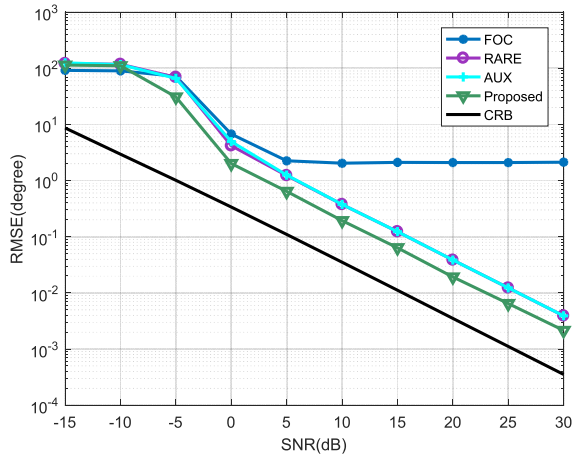

FIGURE 3. RMSEs of DOA estimates versus SNR. 200 snapshots, 500 Monte Carlo trials.

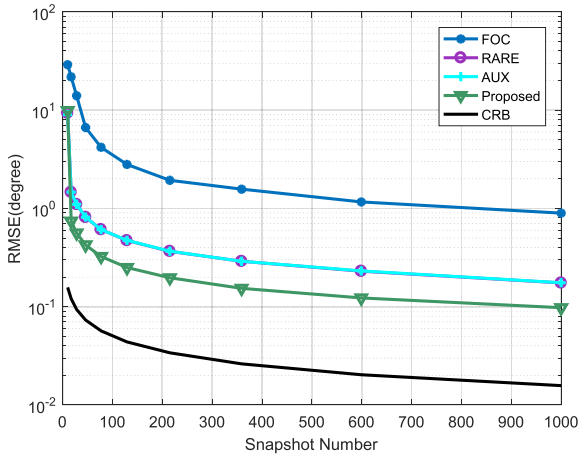

FIGURE 4. RMSEs of DOA estimates versus snapshot number. SNR=10dB, 500 Monte Carlo trials.

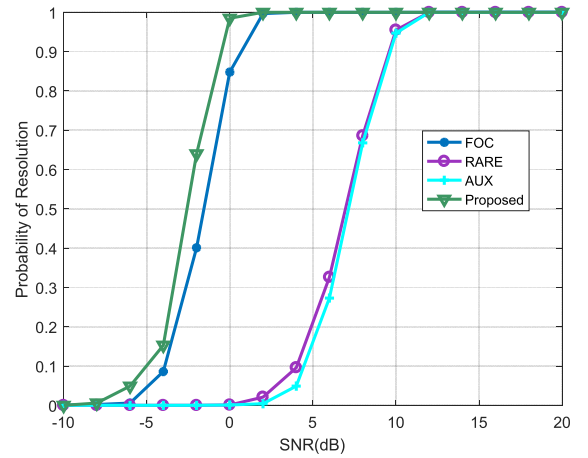

FIGURE 5. Probability of resolution versus SNR. 500 independent trials are realized for each of the four methods.

from −10°, 20° and 50° . The snapshots and the nonzero MCCs are set as 200 and $[1, 0.37 + j0.42, 0.09 - j0.31, 0.08 - j0.12]$, respectively. Figure 3 illustrates the RMSEs of the four algorithms (FOC, RARE, AUX and the proposed one), and the CRB is presented for comparison. According to the results, it is evident that our method achieves a lower SNR threshold at about 0 dB. In addition, it is superior to other three methods and approaches the CRB more closely. The performance of FOC is saturated starting from 5 dB, because of the cumulant matrix estimation errors introduced by limited number of observations.

C. RMSE VERSUS SNAPSHOT NUMBER

In the third experiment, we set the SNR as 10 dB but vary the number of snapshots from 10 to 1000, and the other parameters are assumed the same as the second experiment. Fig. 4 shows that RMSEs of all the algorithms drop gradually with an increase of the number of snapshots. This is due to the fact that better estimates of the covariance and pseudo covariance matrices can be obtained from a larger number of stationary samples. In addition, the RMSE of our algorithm is reasonably close to the corresponding CRB and outperforms other methods.

D. PROBABILITY OF RESOLUTION VERSUS SNR

In the fourth experiment, we investigate the PR of the four algorithms versus SNR. Consider that there are two BPSK sources radiating at −2° and 2°, and the SNR ranges from −10 dB to 20 dB in steps of 2 dB. It can be seen from Figure 5 that the proposed algorithm has the lowest SNR threshold of the full PR, while RARE and AUX have worse resolution as the SNR thresholds are both 12 dB that is much higher than that of our method. This is due to the fact that the noncircular information has been fully utilized to enhance the resolution capability at low SNRs.

E. COMPUTATIONAL COMPLEXITY COMPARISON

In this experiment, we compare the computational loads of the four algorithms. The searching step for DOA estimation

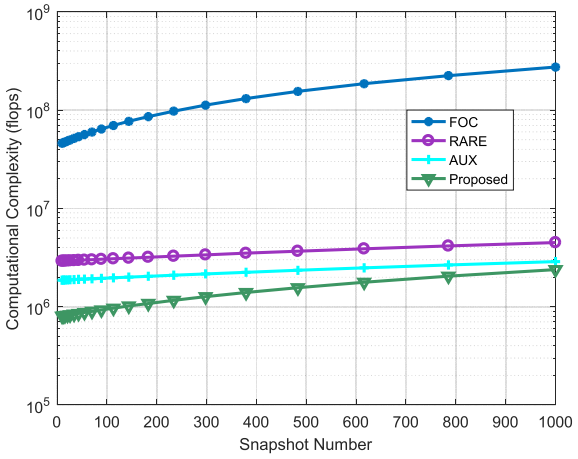

FIGURE 6. Computational complexity of the four methods versus snapshot number.

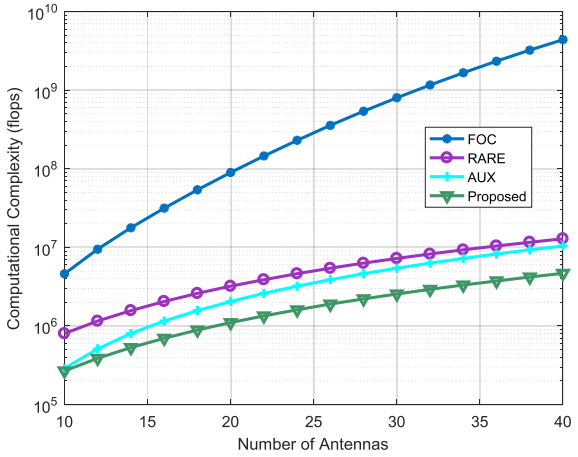

FIGURE 7. Computational complexity of the four methods versus number of antennas.

is fixed at 1°, and the number of snapshots ranges from 10 to 1000. Fig. 6 illustrates the computational burden of these algorithms as a function of the snapshot number. It can be observed that the computational cost of RARE and AUX is slightly higher than that of our method, while FOC takes the most computational load since it has to calculate the fourth order cumulants that involves biquadratic operations.

Next, we assume that the number of snapshots is set as 200 and the antenna elements ranges from 10 to 40. The computational loads of the four algorithms versus the variation of antenna elements is illustrated in Figure 7. Similarly, we can draw the conclusion that the proposed algorithm is most efficient compared with other ones.

VI. CONCLUSION

In this paper, a real-valued direction finding algorithm has been proposed for noncircular sources in the presence of unknown mutual coupling. Exploiting the characteristics of noncircularity and the Toeplitz structure of the mutual coupling matrix, a real-valued RARE based algorithm is proposed to separate the DOAs from other nuisance parameters. Compared with some existing works, our method has improved estimation accuracy and achieved more resolvable signals. The simulation results demonstrate the efficiency and effectiveness of the proposed method for the DOA estimation of noncircular sources under mutual coupling.

APPENDIX
DERIVATION OF CRAMER-RAO BOUND

In the appendix, we derive the corresponding stochastic CRB of DOA estimation for noncircular sources under unknown mutual coupling effect.

Let $\boldsymbol{\Theta} = [\boldsymbol{\theta}^T, \boldsymbol{\psi}^T, \boldsymbol{\kappa}^T, \boldsymbol{\upsilon}^T, \boldsymbol{\mu}^T, \sigma_n^2]$ denotes the real-valued unknown parameter vector, where $\boldsymbol{\theta} = [\theta_1, \ldots, \theta_K]^T$ is the DOA vector, $\boldsymbol{\psi} = [\psi_1, \ldots, \psi_K]^T$ contains the noncircular phases, $\boldsymbol{\kappa} = \mathrm{Re}\{c_1, \ldots, c_{P-1}\}^T$ and $\boldsymbol{\upsilon} = \mathrm{Im}\{c_1, \ldots, c_{P-1}\}^T$ are the real and imaginary parts of the mutual coupling coefficients, $\boldsymbol{\mu} = [\mu_1, \ldots, \mu_K]$ is the $K \times 1$ vector made from $[\mathbf{R}_s]_{i,i}$, $1 \le i \le K$, since it is assumed that the sources are uncorrelated. Suppose that the T samples of $\mathbf{x}(t)$, $t = 1, \ldots, T$ are independent and noncircularly Gaussian distributed. Based on the results in [32] and [33], the Fisher information matrix (FIM) corresponding to the parameter vector $\boldsymbol{\Theta}$ can be written as

$$\mathbf{F}_{m,n} = T \cdot \mathrm{Tr}\left(\frac{\partial \mathbf{R}_{\tilde{\mathbf{x}}}}{\partial \boldsymbol{\Theta}_m} \mathbf{R}_{\tilde{\mathbf{x}}}^{-1} \frac{\partial \mathbf{R}_{\tilde{\mathbf{x}}}}{\partial \boldsymbol{\Theta}_n} \mathbf{R}_{\tilde{\mathbf{x}}}^{-1} \right) \tag{38}$$

herein, $\mathbf{R}_{\tilde{\mathbf{x}}}$ is the extended covariance matrix corresponding to the augmented signal $\tilde{\mathbf{x}}(t) = [\mathbf{x}^T(t), \mathbf{x}^H(t)]^T$, which is formed as

$$\mathbf{R}_{\tilde{\mathbf{x}}} = E\{\tilde{\mathbf{x}}(t)\tilde{\mathbf{x}}^H(t)\} = \tilde{\mathbf{A}}\mathbf{R}_s\tilde{\mathbf{A}}^H + \sigma_n^2\mathbf{I} \tag{39}$$

where $\tilde{\mathbf{A}} = \begin{bmatrix} \mathbf{C}\mathbf{A}\boldsymbol{\Phi} \\ \mathbf{C}^*\mathbf{A}^*\boldsymbol{\Phi}^* \end{bmatrix} = [\tilde{\mathbf{a}}_1, \ldots, \tilde{\mathbf{a}}_K]$, with $\tilde{\mathbf{a}}_k = \begin{bmatrix} e^{j\psi_k}\mathbf{C}\mathbf{a}(\theta_k) \\ e^{-j\psi_k}\mathbf{C}^*\mathbf{a}^*(\theta_k) \end{bmatrix}$.

The FIM for the unknown parameters and their cross terms are derived in detail in the following subsection. Since $\mathbf{F}$ is a symmetric matrix, we only need to find the upper triangular parts of $\mathbf{F}$.

A. FIM WITH RESPECT TO DOA

The partial derivative of the covariance matrix with respect to DOA is of the following form

$$\frac{\partial \mathbf{R}_{\tilde{\mathbf{x}}}}{\partial \theta_m} = \dot{\tilde{\mathbf{A}}}_{\theta_m}\mathbf{R}_s\tilde{\mathbf{A}}^H + \tilde{\mathbf{A}}\mathbf{R}_s\dot{\tilde{\mathbf{A}}}_{\theta_m}^H \tag{40}$$

where $\dot{\tilde{\mathbf{A}}}_{\theta_m} = \partial\tilde{\mathbf{A}}/\partial\theta_m = [\mathbf{0}, \ldots, \partial\tilde{\mathbf{a}}_m/\partial\theta_m, \ldots, \mathbf{0}]$. Note that the nonzero element of $\dot{\tilde{\mathbf{A}}}_{\theta_m}$ only lies in the mth column, thus it can be expressed as

$$\dot{\tilde{\mathbf{A}}}_{\theta_m} = \dot{\tilde{\mathbf{A}}}_{\boldsymbol{\theta}}\mathbf{e}_m\mathbf{e}_m^T \tag{41}$$

herein, $\mathbf{e}_m$ represents the mth column of the identity matrix $\mathbf{I}_{2M}$, and $\dot{\tilde{\mathbf{A}}}_{\boldsymbol{\theta}}$ is the matrix composed of derivatives

$$\dot{\tilde{\mathbf{A}}}_{\boldsymbol{\theta}} = \left[\frac{\partial\tilde{\mathbf{a}}_1}{\partial\theta_1}, \ldots, \frac{\partial\tilde{\mathbf{a}}_K}{\partial\theta_K} \right] \tag{42}$$

Substituting (40) into (38), it can be deduced that

$$\begin{aligned}\mathbf{F}_{\theta_m\theta_n} &= 2T\cdot \mathrm{Re}\left\{\mathrm{Tr}\left\{\mathbf{R}_{\tilde{\mathbf{x}}}^{-1}\dot{\tilde{\mathbf{A}}}_{\boldsymbol{\theta}}\mathbf{e}_m\mathbf{e}_m^T\mathbf{R}_s\tilde{\mathbf{A}}^H\mathbf{R}_{\tilde{\mathbf{x}}}^{-1}\dot{\tilde{\mathbf{A}}}_{\boldsymbol{\theta}}\mathbf{e}_n\mathbf{e}_n^T\mathbf{R}_s\tilde{\mathbf{A}}^H\right\}\right.\\ &\quad\left.+\ \mathrm{Tr}\left\{\mathbf{R}_{\tilde{\mathbf{x}}}^{-1}\dot{\tilde{\mathbf{A}}}_{\boldsymbol{\theta}}\mathbf{e}_m\mathbf{e}_m^T\mathbf{R}_s\tilde{\mathbf{A}}^H\mathbf{R}_{\tilde{\mathbf{x}}}^{-1}\tilde{\mathbf{A}}\mathbf{R}_s\mathbf{e}_n\mathbf{e}_n^T\dot{\tilde{\mathbf{A}}}_{\boldsymbol{\theta}}^H\right\}\right\}\\ &= 2T\cdot Re\left\{\mathbf{e}_m^T\mathbf{R}_s\tilde{\mathbf{A}}^H\mathbf{R}_{\tilde{\mathbf{x}}}^{-1}\dot{\tilde{\mathbf{A}}}_{\boldsymbol{\theta}}\mathbf{e}_n\mathbf{e}_n^T\mathbf{R}_s\tilde{\mathbf{A}}^H\mathbf{R}_{\tilde{\mathbf{x}}}^{-1}\dot{\tilde{\mathbf{A}}}_{\boldsymbol{\theta}}\mathbf{e}_m\right.\\ &\quad\left.+\ \mathbf{e}_m^T\mathbf{R}_s\tilde{\mathbf{A}}^H\mathbf{R}_{\tilde{\mathbf{x}}}^{-1}\tilde{\mathbf{A}}R_s\mathbf{e}_n\mathbf{e}_n^T\dot{\tilde{\mathbf{A}}}_{\boldsymbol{\theta}}^H\mathbf{R}_{\tilde{\mathbf{x}}}^{-1}\dot{\tilde{\mathbf{A}}}_{\boldsymbol{\theta}}\mathbf{e}_m\right\}\end{aligned}\tag{43}$$

Therefore,

$$\begin{aligned}\mathbf{F}_{\boldsymbol{\theta\theta}} &= 2T\cdot Re\{(\mathbf{R}_s\tilde{\mathbf{A}}^H\mathbf{R}_{\tilde{\mathbf{x}}}^{-1}\dot{\tilde{\mathbf{A}}}_{\boldsymbol{\theta}})\odot(\mathbf{R}_s\tilde{\mathbf{A}}^H\mathbf{R}_{\tilde{\mathbf{x}}}^{-1}\dot{\tilde{\mathbf{A}}}_{\boldsymbol{\theta}})^T\\ &\quad+(\mathbf{R}_s\tilde{\mathbf{A}}^H\mathbf{R}_{\tilde{\mathbf{x}}}^{-1}\tilde{\mathbf{A}}R_s)\odot(\dot{\tilde{\mathbf{A}}}_{\boldsymbol{\theta}}^H\mathbf{R}_{\tilde{\mathbf{x}}}^{-1}\dot{\tilde{\mathbf{A}}}_{\boldsymbol{\theta}})^T\}\end{aligned}\tag{44}$$

B. FIM WITH RESPECT TO NONCIRCULAR PHASE

Similarly, the partial derivative of the covariance matrix with respect to noncircular phase is of the following form

$$\frac{\partial\mathbf{R}_{\tilde{\mathbf{x}}}}{\partial\psi_m}=\dot{\tilde{\mathbf{A}}}_{\psi_m}\mathbf{R}_s\tilde{\mathbf{A}}^H+\tilde{\mathbf{A}}R_s\dot{\tilde{\mathbf{A}}}_{\psi_m}^H\tag{45}$$

where $\dot{\tilde{\mathbf{A}}}_{\psi_m}=\partial\tilde{\mathbf{A}}/\partial\psi_m=\left[\mathbf{0},\ldots,\partial\tilde{\mathbf{a}}_m/\partial\psi_m,\ldots,\mathbf{0}\right]$. Note that the nonzero element of $\dot{\tilde{\mathbf{A}}}_{\psi_m}$ only lies in the mth column, thus it can be expressed as

$$\dot{\tilde{\mathbf{A}}}_{\psi_m}=\dot{\tilde{\mathbf{A}}}_{\boldsymbol{\psi}}\mathbf{e}_m\mathbf{e}_m^T\tag{46}$$

herein, $\dot{\tilde{\mathbf{A}}}_{\boldsymbol{\psi}}$ is the matrix composed of derivatives

$$\dot{\tilde{\mathbf{A}}}_{\boldsymbol{\psi}}=\left[\frac{\partial\tilde{\mathbf{a}}_1}{\partial\psi_1},\ldots,\frac{\partial\tilde{\mathbf{a}}_K}{\partial\psi_K}\right]\tag{47}$$

Substituting (45) into (38), it can be deduced that

$$\begin{aligned}\mathbf{F}_{\psi_m\psi_n} &= 2T\cdot \mathrm{Re}\left\{\mathrm{Tr}\left\{\mathbf{R}_{\tilde{\mathbf{x}}}^{-1}\dot{\tilde{\mathbf{A}}}_{\boldsymbol{\psi}}\mathbf{e}_m\,\mathbf{e}_m^T\mathbf{R}_s\tilde{\mathbf{A}}^H\mathbf{R}_{\tilde{\mathbf{x}}}^{-1}\dot{\tilde{\mathbf{A}}}_{\boldsymbol{\psi}}\mathbf{e}_n\mathbf{e}_n^T\mathbf{R}_s\tilde{\mathbf{A}}^H\right\}\right.\\ &\quad\left.+\ \mathrm{Tr}\left\{\mathbf{R}_{\tilde{\mathbf{x}}}^{-1}\dot{\tilde{\mathbf{A}}}_{\boldsymbol{\psi}}\mathbf{e}_m\mathbf{e}_m^T\,\mathbf{R}_s\tilde{\mathbf{A}}^H\mathbf{R}_{\tilde{\mathbf{x}}}^{-1}\tilde{\mathbf{A}}R_s\mathbf{e}_n\mathbf{e}_n^T\dot{\tilde{\mathbf{A}}}_{\boldsymbol{\psi}}^H\right\}\right\}\\ &= 2T\cdot \mathrm{Re}\left\{\mathbf{e}_m^T\mathbf{R}_s\tilde{\mathbf{A}}^H\,\mathbf{R}_{\tilde{\mathbf{x}}}^{-1}\dot{\tilde{\mathbf{A}}}_{\boldsymbol{\psi}}\mathbf{e}_n\mathbf{e}_n^T\mathbf{R}_s\tilde{\mathbf{A}}^H\mathbf{R}_{\tilde{\mathbf{x}}}^{-1}\dot{\tilde{\mathbf{A}}}_{\boldsymbol{\psi}}\mathbf{e}_m\right.\\ &\quad\left.+\ \mathbf{e}_m^T\mathbf{R}_s\tilde{\mathbf{A}}^H\,\mathbf{R}_{\tilde{\mathbf{x}}}^{-1}\tilde{\mathbf{A}}R_s\mathbf{e}_n\mathbf{e}_n^T\dot{\tilde{\mathbf{A}}}_{\boldsymbol{\psi}}^H\mathbf{R}_{\tilde{\mathbf{x}}}^{-1}\dot{\tilde{\mathbf{A}}}_{\boldsymbol{\psi}}\mathbf{e}_m\right\}\end{aligned}\tag{48}$$

Then,

$$\begin{aligned}\mathbf{F}_{\boldsymbol{\psi\psi}} &= 2T\cdot \mathrm{Re}\left\{\left(\mathbf{R}_s\tilde{\mathbf{A}}^H\mathbf{R}_{\tilde{\mathbf{x}}}^{-1}\dot{\tilde{\mathbf{A}}}_{\boldsymbol{\psi}}\right)\odot\left(\mathbf{R}_s\tilde{\mathbf{A}}^H\mathbf{R}_{\tilde{\mathbf{x}}}^{-1}\dot{\tilde{\mathbf{A}}}_{\boldsymbol{\psi}}\right)^T\right.\\ &\quad\left.+\left(\mathbf{R}_s\tilde{\mathbf{A}}^H\mathbf{R}_{\tilde{\mathbf{x}}}^{-1}\tilde{\mathbf{A}}\mathbf{R}_s\right)\odot\left(\dot{\tilde{\mathbf{A}}}_{\boldsymbol{\psi}}^H\mathbf{R}_{\tilde{\mathbf{x}}}^{-1}\dot{\tilde{\mathbf{A}}}_{\boldsymbol{\psi}}\right)^T\right\}\end{aligned}\tag{49}$$

C. FIM WITH RESPECT TO MCC

The partial derivative with respect to the real part of MCC is of the following form

$$\frac{\partial\mathbf{R}_{\tilde{\mathbf{x}}}}{\partial\kappa_m}=\dot{\tilde{\mathbf{A}}}_{\kappa_m}\mathbf{R}_s\tilde{\mathbf{A}}^H+\tilde{\mathbf{A}}\mathbf{R}_s\dot{\tilde{\mathbf{A}}}_{\kappa_m}^H\tag{50}$$

where $\dot{\tilde{\mathbf{A}}}_{\kappa_m}=\partial\tilde{\mathbf{A}}/\partial\kappa_m=\left[\mathbf{0},\ldots,\partial\tilde{\mathbf{a}}_m/\partial\kappa_m,\ldots,\mathbf{0}\right]$. Note that the nonzero element of $\dot{\tilde{\mathbf{A}}}_{\kappa_m}$ only lies in the mth column, thus it can be expressed as

$$\dot{\tilde{\mathbf{A}}}_{\kappa_m}=\begin{bmatrix}\dfrac{\partial\mathbf{C}}{\partial\kappa_m}\mathbf{A}\boldsymbol{\Phi}\\ \dfrac{\partial\mathbf{C}^*}{\partial\kappa_m}\mathbf{A}^*\boldsymbol{\Phi}^*\end{bmatrix}\tag{51}$$

Therefore, we can obtain that

$$\begin{aligned}\mathbf{F}_{\kappa_m\kappa_n} &= 2T\cdot \mathrm{Re}\left\{\mathrm{Tr}\left\{\mathbf{R}_{\tilde{\mathbf{x}}}^{-1}\dot{\tilde{\mathbf{A}}}_{\kappa_m}\mathbf{R}_s\tilde{\mathbf{A}}^H\mathbf{R}_{\tilde{\mathbf{x}}}^{-1}\dot{\tilde{\mathbf{A}}}_{\kappa_n}\mathbf{R}_s\tilde{\mathbf{A}}^H\right\}\right.\\ &\quad\left.+\ \mathrm{Tr}\left\{\mathbf{R}_{\tilde{\mathbf{x}}}^{-1}\dot{\tilde{\mathbf{A}}}_{\kappa_m}\mathbf{R}_s\tilde{\mathbf{A}}^H\,\mathbf{R}_{\tilde{\mathbf{x}}}^{-1}\tilde{\mathbf{A}}R_s\dot{\tilde{\mathbf{A}}}_{\kappa_n}^H\right\}\right\}\end{aligned}\tag{52}$$

Likewise, $\mathbf{F}_{\upsilon_m\upsilon_n}$, $\mathbf{F}_{\kappa_m\upsilon_n}$ and $\mathbf{F}_{\upsilon_m\kappa_n}$ can be obtained by substituting $\partial\mathbf{R}_{\tilde{\mathbf{x}}}/\partial\kappa_m$ and $\partial\mathbf{R}_{\tilde{\mathbf{x}}}/\partial\upsilon_m$ into (38).

D. FIM WITH RESPECT TO SIGNAL COVARIANCE

Since the noncircular sources are uncorrelated with each other, then $\mathbf{R}_{\tilde{\mathbf{x}}}$ reduces to

$$\mathbf{R}_{\tilde{\mathbf{x}}}=\sum_{k=1}^{K}\mu_k\tilde{\mathbf{a}}_k\tilde{\mathbf{a}}_k^H+\sigma_n^2\mathbf{I}\tag{53}$$

Therefore, the partial derivative of the covariance matrix with respect to signal covariance elements is of the following form

$$\frac{\partial\mathbf{R}_{\tilde{\mathbf{x}}}}{\partial\mu_k}=\tilde{\mathbf{a}}_k\tilde{\mathbf{a}}_k^H\tag{54}$$

Substituting (54) into (38), it can be deduced that

$$\begin{aligned}\mathbf{F}_{\mu_m\mu_n} &= T\cdot\mathrm{Tr}\{\mathbf{R}_{\tilde{\mathbf{x}}}^{-1}\tilde{\mathbf{a}}_m\tilde{\mathbf{a}}_m^H\mathbf{R}_{\tilde{\mathbf{x}}}^{-1}\tilde{\mathbf{a}}_n\tilde{\mathbf{a}}_n^H\}\\ &= T\cdot\mathrm{Tr}\{\mathbf{e}_m^T\tilde{\mathbf{A}}^H\mathbf{R}_{\tilde{\mathbf{x}}}^{-1}\tilde{\mathbf{A}}e_n\mathbf{e}_n^T\tilde{\mathbf{A}}^H\mathbf{R}_{\tilde{\mathbf{x}}}^{-1}\tilde{\mathbf{A}}e_m\}\end{aligned}\tag{55}$$

Then,

$$\mathbf{F}_{\boldsymbol{\mu\mu}}=T\cdot(\tilde{\mathbf{A}}^H\mathbf{R}_{\tilde{\mathbf{x}}}^{-1}\tilde{\mathbf{A}})\odot(\tilde{\mathbf{A}}^H\mathbf{R}_{\tilde{\mathbf{x}}}^{-1}\tilde{\mathbf{A}})^T\tag{56}$$

E. DOA AND NONCIRCULAR PHASE CROSS TERM

Analogously, by applying (40) and (45), it can be obtained that

$$\begin{aligned}\mathbf{F}_{\theta_m\psi_n} &= 2T\cdot \mathrm{Re}\left\{\mathbf{e}_m^T\mathbf{R}_s\tilde{\mathbf{A}}^H\mathbf{R}_{\tilde{\mathbf{x}}}^{-1}\dot{\tilde{\mathbf{A}}}_{\boldsymbol{\theta}}\mathbf{e}_n\mathbf{e}_n^T\,\mathbf{R}_s\tilde{\mathbf{A}}^H\mathbf{R}_{\tilde{\mathbf{x}}}^{-1}\dot{\tilde{\mathbf{A}}}_{\boldsymbol{\psi}}\mathbf{e}_m\right.\\ &\quad\left.+\ \mathbf{e}_m^T\mathbf{R}_s\tilde{\mathbf{A}}^H\,\mathbf{R}_{\tilde{\mathbf{x}}}^{-1}\tilde{\mathbf{A}}R_s\mathbf{e}_n\mathbf{e}_n^T\dot{\tilde{\mathbf{A}}}_{\boldsymbol{\psi}}^H\mathbf{R}_{\tilde{\mathbf{x}}}^{-1}\dot{\tilde{\mathbf{A}}}_{\boldsymbol{\theta}}\mathbf{e}_m\right\}\end{aligned}\tag{57}$$

Consequently,

$$\begin{aligned}\mathbf{F}_{\boldsymbol{\theta\psi}} &= 2T\cdot \mathrm{Re}\{(\mathbf{R}_s\tilde{\mathbf{A}}^H\mathbf{R}_{\tilde{\mathbf{x}}}^{-1}\dot{\tilde{\mathbf{A}}}_{\boldsymbol{\theta}})\odot(\mathbf{R}_s\tilde{\mathbf{A}}^H\mathbf{R}_{\tilde{\mathbf{x}}}^{-1}\dot{\tilde{\mathbf{A}}}_{\boldsymbol{\psi}})^T\\ &\quad+(\mathbf{R}_s\tilde{\mathbf{A}}^H\mathbf{R}_{\tilde{\mathbf{x}}}^{-1}\tilde{\mathbf{A}}R_s)\odot(\dot{\tilde{\mathbf{A}}}_{\boldsymbol{\psi}}^H\mathbf{R}_{\tilde{\mathbf{x}}}^{-1}\dot{\tilde{\mathbf{A}}}_{\boldsymbol{\theta}})^T\}\end{aligned}\tag{58}$$

F. DOA AND MCC CROSS TERM

By applying (40) and (50), we have

$$\mathbf{F}_{\theta_m\kappa_n} = 2T \cdot \mathrm{Re}\left\{\mathbf{e}_m^T\mathbf{R}_s\tilde{\mathbf{A}}^H\mathbf{R}_{\tilde{\mathbf{x}}}^{-1}\dot{\tilde{\mathbf{A}}}_{\kappa_n}\mathbf{R}_s\tilde{\mathbf{A}}^H\mathbf{R}_{\tilde{\mathbf{x}}}^{-1}\dot{\tilde{\mathbf{A}}}_{\boldsymbol{\theta}}\mathbf{e}_m + \mathbf{e}_m^T\mathbf{R}_s\tilde{\mathbf{A}}^H\,\mathbf{R}_{\tilde{\mathbf{x}}}^{-1}\tilde{\mathbf{A}}\mathbf{R}_s\dot{\tilde{\mathbf{A}}}_{\kappa_n}^H\mathbf{R}_{\tilde{\mathbf{x}}}^{-1}\dot{\tilde{\mathbf{A}}}_{\boldsymbol{\theta}}\mathbf{e}_m\right\} \quad (59)$$

$$\mathbf{F}_{\boldsymbol{\theta}\kappa_n} = 2T \cdot \mathrm{Re}\left\{\mathrm{diag}\{\mathbf{R}_s\tilde{\mathbf{A}}^H\mathbf{R}_{\tilde{\mathbf{x}}}^{-1}\dot{\tilde{\mathbf{A}}}_{\kappa_n}\mathbf{R}_s\tilde{\mathbf{A}}^H\mathbf{R}_{\tilde{\mathbf{x}}}^{-1}\dot{\tilde{\mathbf{A}}}_{\boldsymbol{\theta}}\} + \mathrm{diag}\{\mathbf{R}_s\tilde{\mathbf{A}}^H\mathbf{R}_{\tilde{\mathbf{x}}}^{-1}\tilde{\mathbf{A}}\mathbf{R}_s\dot{\tilde{\mathbf{A}}}_{\kappa_n}^H\mathbf{R}_{\tilde{\mathbf{x}}}^{-1}\dot{\tilde{\mathbf{A}}}_{\boldsymbol{\theta}}\}\right\} \quad (60)$$

The DOA and real part MCC cross term can be expressed as

$$\mathbf{F}_{\boldsymbol{\theta\kappa}} = \left[\mathbf{F}_{\boldsymbol{\theta}\kappa_1}, \ldots, \mathbf{F}_{\boldsymbol{\theta}\kappa_P}\right] \quad (61)$$

And $\mathbf{F}_{\boldsymbol{\theta\upsilon}}$ can be obtained in a similar way.

G. DOA AND SIGNAL COVARIANCE CROSS TERM

By applying (40) and (54), we have

$$\begin{aligned}\mathbf{F}_{\theta_m\mu_n} &= T \cdot \mathrm{Tr}\left\{\mathbf{R}_{\tilde{\mathbf{x}}}^{-1}\left(\dot{\tilde{\mathbf{A}}}_{\theta_m}\mathbf{R}_s\tilde{\mathbf{A}}^H + \tilde{\mathbf{A}}R_s\dot{\tilde{\mathbf{A}}}_{\theta_m}^H\right)\mathbf{R}_{\tilde{\mathbf{x}}}^{-1}\tilde{\mathbf{a}}_n\tilde{\mathbf{a}}_n^H\right\} \\ &= 2T \cdot Re\left\{\tilde{\mathbf{a}}_n^H\mathbf{R}_{\tilde{\mathbf{x}}}^{-1}\dot{\tilde{\mathbf{A}}}_{\boldsymbol{\theta}}\mathbf{e}_m\mathbf{e}_m^T\mathbf{R}_s\tilde{\mathbf{A}}^H\,\mathbf{R}_{\tilde{\mathbf{x}}}^{-1}\tilde{\mathbf{a}}_n\right\} \\ &= 2T \cdot Re\left\{\mathbf{e}_m^T\mathbf{R}_s\tilde{\mathbf{A}}^H\,\mathbf{R}_{\tilde{\mathbf{x}}}^{-1}\tilde{\mathbf{A}}e_n\mathbf{e}_n^T\tilde{\mathbf{A}}^H\mathbf{R}_{\tilde{\mathbf{x}}}^{-1}\dot{\tilde{\mathbf{A}}}_{\boldsymbol{\theta}}\mathbf{e}_m\right\} \quad (62)\end{aligned}$$

Thus,

$$\mathbf{F}_{\boldsymbol{\theta\mu}} = 2T \cdot Re\left\{\left(\mathbf{R}_s\tilde{\mathbf{A}}^H\mathbf{R}_{\tilde{\mathbf{x}}}^{-1}\tilde{\mathbf{A}}\right) \odot \left(\tilde{\mathbf{A}}^H\mathbf{R}_{\tilde{\mathbf{x}}}^{-1}\dot{\tilde{\mathbf{A}}}_{\boldsymbol{\theta}}\right)^T\right\} \quad (63)$$

H. NONCIRCULAR PHASE AND MCC CROSS TERM

Based on (45) and (50), we have

$$\mathbf{F}_{\psi_m\kappa_n} = 2T \cdot \mathrm{Re}\left\{\mathbf{e}_m^T\mathbf{R}_s\tilde{\mathbf{A}}^H\mathbf{R}_{\tilde{\mathbf{x}}}^{-1}\dot{\tilde{\mathbf{A}}}_{\kappa_n}\mathbf{R}_s\tilde{\mathbf{A}}^H\mathbf{R}_{\tilde{\mathbf{x}}}^{-1}\dot{\tilde{\mathbf{A}}}_{\boldsymbol{\psi}}\mathbf{e}_m + \mathbf{e}_m^T\mathbf{R}_s\tilde{\mathbf{A}}^H\,\mathbf{R}_{\tilde{\mathbf{x}}}^{-1}\tilde{\mathbf{A}}\mathbf{R}_s\dot{\tilde{\mathbf{A}}}_{\kappa_n}^H\mathbf{R}_{\tilde{\mathbf{x}}}^{-1}\dot{\tilde{\mathbf{A}}}_{\boldsymbol{\psi}}\mathbf{e}_m\right\} \quad (64)$$

Therefore,

$$\mathbf{F}_{\boldsymbol{\psi}\kappa_n} = 2T \cdot \mathrm{Re}\left\{\mathrm{diag}\{\mathbf{R}_s\tilde{\mathbf{A}}^H\mathbf{R}_{\tilde{\mathbf{x}}}^{-1}\dot{\tilde{\mathbf{A}}}_{\kappa_n}\mathbf{R}_s\tilde{\mathbf{A}}^H\mathbf{R}_{\tilde{\mathbf{x}}}^{-1}\dot{\tilde{\mathbf{A}}}_{\boldsymbol{\psi}}\} + \mathrm{diag}\{\mathbf{R}_s\tilde{\mathbf{A}}^H\mathbf{R}_{\tilde{\mathbf{x}}}^{-1}\tilde{\mathbf{A}}\mathbf{R}_s\dot{\tilde{\mathbf{A}}}_{\kappa_n}^H\mathbf{R}_{\tilde{\mathbf{x}}}^{-1}\dot{\tilde{\mathbf{A}}}_{\boldsymbol{\psi}}\}\right\} \quad (65)$$

I. NONCIRCULAR PHASE AND SIGNAL COVARIANCE CROSS TERM

Substituting (45) into (54), it can be deduced that

$$\mathbf{F}_{\psi_m\mu_n} = 2T \cdot \mathrm{Re}\left\{\mathbf{e}_m^T\mathbf{R}_s\tilde{\mathbf{A}}^H\mathbf{R}_{\tilde{\mathbf{x}}}^{-1}\tilde{\mathbf{A}}e_n\mathbf{e}_n^T\tilde{\mathbf{A}}^H\mathbf{R}_{\tilde{\mathbf{x}}}^{-1}\dot{\tilde{\mathbf{A}}}_{\boldsymbol{\psi}}\mathbf{e}_m\right\} \quad (66)$$

and

$$\mathbf{F}_{\boldsymbol{\psi\mu}} = 2T \cdot \mathrm{Re}\left\{\left(\mathbf{R}_s\tilde{\mathbf{A}}^H\mathbf{R}_{\tilde{\mathbf{x}}}^{-1}\tilde{\mathbf{A}}\right) \odot \left(\tilde{\mathbf{A}}^H\mathbf{R}_{\tilde{\mathbf{x}}}^{-1}\dot{\tilde{\mathbf{A}}}_{\boldsymbol{\psi}}\right)^T\right\} \quad (67)$$

J. MCC AND SIGNAL COVARIANCE CROSS TERM

Based on (50) and (54), we have

$$\mathbf{F}_{\kappa_m\mu_n} = 2T \cdot \mathrm{Re}\left\{\tilde{\mathbf{a}}_n^H\,\mathbf{R}_{\tilde{\mathbf{x}}}^{-1}\dot{\tilde{\mathbf{A}}}_{\kappa_m}\,\mathbf{R}_s\tilde{\mathbf{A}}^H\mathbf{R}_{\tilde{\mathbf{x}}}^{-1}\tilde{\mathbf{a}}_n\right\} \quad (68)$$

Then, $\mathbf{F}_{\boldsymbol{\kappa\mu}}$, $\mathbf{F}_{\boldsymbol{\upsilon\mu}}$, $\mathbf{F}_{\boldsymbol{\mu\kappa}}$ and $\mathbf{F}_{\boldsymbol{\mu\upsilon}}$ can be readily obtained.

Moreover, it is obvious that the noise power is decoupled with other unknown parameters. Therefore, the cross terms with respect to σ_n^2 are all zeros.

Therefore, taking the above results together, we can formulate the FIM as the following form

$$\mathbf{F} = \begin{bmatrix} \mathbf{F}_{\boldsymbol{\theta\theta}} & \mathbf{F}_{\boldsymbol{\theta\psi}} & \mathbf{F}_{\boldsymbol{\theta\kappa}} & \mathbf{F}_{\boldsymbol{\theta\upsilon}} & \mathbf{F}_{\boldsymbol{\theta\mu}} & \mathbf{0} \\ \mathbf{F}_{\boldsymbol{\psi\theta}} & \mathbf{F}_{\boldsymbol{\psi\psi}} & \mathbf{F}_{\boldsymbol{\psi\kappa}} & \mathbf{F}_{\boldsymbol{\psi\upsilon}} & \mathbf{F}_{\boldsymbol{\psi\mu}} & \mathbf{0} \\ \mathbf{F}_{\boldsymbol{\kappa\theta}} & \mathbf{F}_{\boldsymbol{\kappa\psi}} & \mathbf{F}_{\boldsymbol{\kappa\kappa}} & \mathbf{F}_{\boldsymbol{\kappa\upsilon}} & \mathbf{F}_{\boldsymbol{\kappa\mu}} & \mathbf{0} \\ \mathbf{F}_{\boldsymbol{\upsilon\theta}} & \mathbf{F}_{\boldsymbol{\upsilon\psi}} & \mathbf{F}_{\boldsymbol{\upsilon\kappa}} & \mathbf{F}_{\boldsymbol{\upsilon\upsilon}} & \mathbf{F}_{\boldsymbol{\upsilon\mu}} & \mathbf{0} \\ \mathbf{F}_{\boldsymbol{\mu\theta}} & \mathbf{F}_{\boldsymbol{\mu\psi}} & \mathbf{F}_{\boldsymbol{\mu\kappa}} & \mathbf{F}_{\boldsymbol{\mu\upsilon}} & \mathbf{F}_{\boldsymbol{\mu\mu}} & \mathbf{0} \\ \mathbf{0} & \mathbf{0} & \mathbf{0} & \mathbf{0} & \mathbf{0} & \mathbf{F}_{\sigma_n^2\sigma_n^2} \end{bmatrix} \quad (69)$$

Subsequently, the CRB for DOA parameters is defined as:

$$CRB_{\boldsymbol{\theta}} = \sqrt{\frac{1}{K}\sum_{k=1}^{K}\left[\mathbf{F}^{-1}\right]_{kk}} \quad (70)$$

REFERENCES

[1] L. Wan, X. Kong, and F. Xia, "Joint range-Doppler-angle estimation for intelligent tracking of moving aerial targets," *IEEE Internet Things J.*, vol. 5, no. 3, pp. 1625–1636, Jun. 2018.

[2] X. Wu, W.-P. Zhu, J. Yan, and Z. Zhang, "Two sparse-based methods for off-grid direction-of-arrival estimation," *Signal Process.*, vol. 142, pp. 87–95, Jan. 2018.

[3] H. Abeida and J.-P. Delmas, "MUSIC-like estimation of direction of arrival for noncircular sources," *IEEE Trans. Signal Process.*, vol. 54, no. 7, pp. 2678–2690, Jul. 2006.

[4] H. Abeida and J. P. Delmas, "Statistical performance of MUSIC-like algorithms in resolving noncircular sources," *IEEE Trans. Signal Process.*, vol. 56, no. 9, pp. 4317–4329, Sep. 2008.

[5] Z. Dai, B. Ba, W. Cui, and Y. Sun, "Computational efficient two-dimension DOA estimation for incoherently distributed noncircular sources with automatic pairing," *IEEE Access*, vol. 5, pp. 20249–20259, 2017.

[6] J. Liu, W. Xie, Q. Wan, and G. Gui, "Robust widely linear beamforming via the techniques of iterative QCQP and shrinkage for steering vector estimation," *IEEE Access*, vol. 6, pp. 17143–17152, 2018.

[7] L. Wan, G. Han, L. Shu, S. Chan, and T. Zhu, "The application of DOA estimation approach in patient tracking systems with high patient density," *IEEE Trans. Ind. Informat.*, vol. 12, no. 6, pp. 2353–2364, Dec. 2016.

[8] P. P. J. Schreier and P. L. L. Scharf, *Statistical Signal Processing of Complex-Valued Data: The Theory of Improper and Noncircular Signals*. New York, NY, USA: Cambridge Univ. Press, 2010.

[9] F. Gao, A. Nallanathan, and Y. Wang, "Improved MUSIC under the coexistence of both circular and noncircular sources," *IEEE Trans. Signal Process.*, vol. 56, no. 7, pp. 3033–3038, Jul. 2008.

[10] H. Chen, C. Hou, W. Liu, W.-P. Zhu, and M. N. S. Swamy, "Efficient two-dimensional direction-of-arrival estimation for a mixture of circular and noncircular sources," *IEEE Sensors J.*, vol. 16, no. 8, pp. 2527–2536, Apr. 2016.

[11] J. Liu, Z. Huang, and Y. Zhou, "Extended 2q-MUSIC algorithm for noncircular signals," *Signal Process.*, vol. 88, pp. 1327–1339, Jun. 2008.

[12] Z.-M. Liu, Z.-T. Huang, Y.-Y. Zhou, and J. Liu, "Direction-of-arrival estimation of noncircular signals via sparse representation," *IEEE Trans. Aerosp. Electron. Syst.*, vol. 48, no. 3, pp. 2690–2698, Jul. 2012.

[13] G. Zheng, J. Tang, and X. Yang, "ESPRIT and unitary ESPRIT algorithms for coexistence of circular and noncircular signals in bistatic MIMO radar," *IEEE Access*, vol. 4, pp. 7232–7240, 2016.

[14] J. Xie, H. Tao, X. Rao, and J. Su, "Efficient method of passive localization for near-field noncircular sources," *IEEE Antennas Wireless Propag. Lett.*, vol. 14, pp. 1223–1226, 2015.

[15] J. Xie, H. Tao, X. Rao, and J. Su, "Real-valued localisation algorithm for near-field non-circular sources," *Electron. Lett.*, vol. 51, no. 17, pp. 1330–1331, 2015.
[16] B. C. Ng and C. M. S. See, "Sensor-array calibration using a maximum-likelihood approach," *IEEE Trans. Antennas Propag.*, vol. 44, no. 6, pp. 827–835, Jun. 1996.
[17] C. M. S. See, "Sensor array calibration in the presence of mutual coupling and unknown sensor gains and phases," *Electron. Lett.*, vol. 30, no. 5, pp. 373–374, Mar. 1994.
[18] B. Friedlander and A. J. Weiss, "Direction finding in the presence of mutual coupling," *IEEE Trans. Antennas Propag.*, vol. 39, no. 3, pp. 273–284, Mar. 1991.
[19] Z. Ye, J. Dai, X. Xu, and X. Wu, "DOA estimation for uniform linear array with mutual coupling," *IEEE Trans. Aerosp. Electron. Syst.*, vol. 45, no. 1, pp. 280–288, Jan. 2009.
[20] Z. Ye and C. Liu, "On the resiliency of MUSIC direction finding against antenna sensor coupling," *IEEE Trans. Antennas Propag.*, vol. 56, no. 2, pp. 371–380, Feb. 2008.
[21] X. Xu, Z. Ye, and Y. Zhang, "DOA estimation for mixed signals in the presence of mutual coupling," *IEEE Trans. Signal Process.*, vol. 57, no. 9, pp. 3523–3532, Sep. 2009.
[22] C. Liu, Z. Ye, and Y. Zhang, "DOA estimation based on fourth-order cumulants with unknown mutual coupling," *Signal Process.*, vol. 89, pp. 1819–1843, Sep. 2009.
[23] B. Liao, Z.-G. Zhang, and S.-C. Chan, "DOA estimation and tracking of ULAs with mutual coupling," *IEEE Trans. Aerosp. Electron. Syst.*, vol. 48, no. 1, pp. 891–905, Jan. 2012.
[24] M. Pesavento, A. B. Gershman, and K. M. Wong, "Direction finding in partly calibrated sensor arrays composed of multiple subarrays," *IEEE Trans. Signal Process.*, vol. 50, no. 9, pp. 2103–2115, Sep. 2002.
[25] S. A. Elkader, A. B. Gershman, and K. M. Wong, "Rank reduction direction-of-arrival estimators with an improved robustness against sub-array orientation errors," *IEEE Trans. Signal Process.*, vol. 54, no. 5, pp. 1951–1955, May 2006.
[26] B. Liao and S. Chan, "A cumulant-based approach for direction finding in the presence of mutual coupling," *Signal Process.*, vol. 104, pp. 197–202, Nov. 2014.
[27] J. Xie, H. Tao, X. Rao, and J. Su, "Localization of mixed far-field and near-field sources under unknown mutual coupling," *Digit. Signal Process.*, vol. 50, pp. 229–239, Mar. 2016.
[28] Z. T. Huang, Z. M. Liu, J. Liu, and Y. Y. Zhou, "Performance analysis of MUSIC for non-circular signals in the presence of mutual coupling," *IET Radar, Sonar Navigat.*, vol. 4, no. 5, pp. 703–711, Oct. 2010.
[29] M. Haardt and J. A. Nossek, "Unitary ESPRIT: How to obtain increased estimation accuracy with a reduced computational burden," *IEEE Trans. Signal Process.*, vol. 43, no. 5, pp. 1232–1242, May 1995.
[30] N. Yilmazer, J. Koh, and T. K. Sarkar, "Utilization of a unitary transform for efficient computation in the matrix pencil method to find the direction of arrival," *IEEE Trans. Antennas Propag.*, vol. 54, no. 1, pp. 175–181, Jan. 2006.
[31] F.-G. Yan, S. Liu, J. Wang, M. Jin, and Y. Shen, "Fast DOA estimation using co-prime array," *Electron. Lett.*, vol. 54, no. 7, pp. 409–410, May 2018.
[32] P. Stoica, E. G. Larsson, and A. B. Gershman, "The stochastic CRB for array processing: A textbook derivation," *IEEE Signal Process. Lett.*, vol. 8, no. 5, pp. 148–150, May 2001.
[33] H. Abeida and J. P. Delmas, "Direct derivation of the stochastic CRB of DOA estimation for rectilinear sources," *IEEE Signal Process. Lett.*, vol. 24, no. 10, pp. 1522–1526, Oct. 2017.

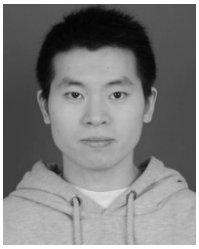

JIAN XIE received the M.Sc. and Ph.D. degrees from the School of Electronic Engineering, Xidian University, in 2012 and 2015, respectively. He is currently an Assistant Professor with Northwestern Polytechnical University. His research interests include antenna array processing and radar signal processing.

LING WANG received the B.Sc., M.Sc., and Ph.D. degrees from Xidian University, Xi'an, China, in 1999, 2002, and 2004, respectively, all in electronic engineering. From 2004 to 2007, he was with Siemens and Nokia Siemens Networks. Since 2007, he has been with the School of Electronic and Information, Northwestern Polytechnical University, Xi'an, and was promoted to a Professor in 2012. His current research interests include array processing and smart antennas, wideband communications, cognitive radio, adaptive antijamming for satellite communications, satellite navigation, and date link systems.

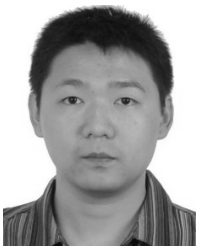

YUEXIAN WANG received the B.S. degree in electronics and information engineering from Northwestern Polytechnical University, China, in 2006, and the M.S. (Eng.) and Ph.D. degrees in electrical and electronic engineering from The University of Adelaide, Australia, in 2012 and 2015, respectively. From 2015 to 2017, he was a Post-Doctoral Fellow at The University of Adelaide. Since 2018, he has been with the School of Electronics and Information, Northwestern Polytechnical University, China. His current research interests include array signal processing, compressed sensing, tensor decomposition, and their applications to radar, sonar, and wireless communications.